

24 **Abstract.** Target identification remains a crucial challenge in drug development. To enable
25 unbiased detection of proteins and pathways that have a causal role in disease pathogenesis
26 or progression, we propose proteome-by-phenome Mendelian Randomisation (P²MR). We
27 first detected genetic variants associated with plasma concentration of 249 proteins. We
28 then used 64 replicated variants in two-sample Mendelian Randomisation to quantify
29 evidence of a causal role for each protein across 846 phenotypes: this yielded 509 robust
30 protein-outcome links. P²MR provides substantial promise for drug target prioritisation. We
31 provide confirmatory evidence for a causal role for the proteins encoded at multiple
32 cardiovascular disease risk loci (*FGF5*, *IL6R*, *LPL*, *LTA*), and discovered that intestinal fatty
33 acid binding protein (*FABP2*) contributes to disease pathogenesis. Additionally, we find and
34 replicate evidence for a causal role of tyrosine-protein phosphatase non-receptor type
35 substrate 1 (*SHPS1*; *SIRPA*) in schizophrenia. Our results provide specific prediction of the
36 effects of changes of plasma protein concentration on complex phenotypes in humans.

37

38 An initial goal of drug development is the identification of targets – in most cases, proteins –
39 whose interaction with a drug ameliorates the development, progression, or symptoms of
40 disease. After some success, the rate of discovery of new targets has not accelerated despite
41 substantially increased investment (Munos, 2009). A large proportion of drugs fail at the last
42 stages of development – clinical trials – because their targets do not alter whole-organism
43 phenotypes as expected from pre-clinical research (Arrowsmith, 2011).

44

45 Preclinical science is engaging with increasingly complex systems in which prediction of the
46 effects of an intervention is ever more difficult (Civelek & Lusic, 2014). The ability to cut
47 through complexity to distinguish factors that modulate whole-organism phenotypes is a
48 major advantage of genetic (Baillie, 2014) and functional genomic (Baillie et al., 2018)
49 approaches to drug development. Nevertheless, genetic associations with disease are not
50 immediately interpretable (MacArthur et al., 2017): most disease-associated variants fail to
51 alter protein-coding sequence, but instead alter protein levels via often poorly understood
52 molecular mechanisms.

53

54 A subset of disease states have been studied with adequately-powered genome-wide
55 association (GWA) studies (Finan et al., 2017). From these, persuasive evidence already
56 exists for the utility of using genetic and genomic techniques to inform drug development:
57 the presence of genetic evidence in support of a protein could double the probability of
58 success in clinical trials for drugs targeting that protein (M. R. Nelson et al., 2015). In a
59 recent study, 12% of all targets for licenced drugs could be rediscovered using GWA studies
60 (Finan et al., 2017). However, these GWA study approaches generally rely on measures of
61 proximity of a disease-associated genetic variant to a protein-coding gene, and proximity
62 alone does not imply causality.

63

64 Mendelian Randomisation (MR) uses genetic variants to provide an estimate of the effect of
65 an exposure on an outcome, using the randomness of assignment of genotype to remove the
66 effects of unmeasured confounding (Smith & Ebrahim, 2003). The approach is analogous to

67 a naturally-occurring randomised control trial. When a genetic variant predicts the
68 abundance of a mediator, MR tests the hypothesis that this mediator plays a causal role in
69 disease risk. This is possible because the patient or participant was effectively randomised at
70 conception to a genetically-determined level of that mediator. Under this model, it is possible
71 to use population level genetic information to draw causal inference from observational data.
72 However, there are, as with any study, unverifiable assumptions with this study design: a
73 major concern is that alternative causal pathways may link the instrumental variable (here,
74 the DNA variant) to the phenotype (the disease outcome). In a clinical trial this would be
75 analogous to a drug influencing a disease through a different pathway than via its reported
76 target. In MR, addressing the risk of alternative causal pathways is of great practical
77 importance in order to avoid pursuing drugs that target an irrelevant molecular entity, and
78 hence that have no beneficial effect. In order to address this, we limited ourselves to using
79 locally-acting pQTLs as instrumental variables. We believe this approach provides stronger
80 supporting evidence for causation than relying on proximity of a disease-associated genetic
81 variant to a gene, or using mRNA abundance as a proxy for protein abundance (Mirauta et al.,
82 2018).

83

84 Due to recent advances in proteomic technologies, the availability of pQTL data has
85 increased dramatically in recent years (Folkersen et al., 2017; Suhre et al., 2017; Sun et al.,
86 2018; Yao et al., 2018). A number of these studies attempt to infer causality using MR and
87 similar techniques. In our approach, we applied pQTL based MR in a data-driven manner
88 across the full range of phenotypes available in GeneAtlas (UK Biobank (Canela-Xandri,
89 Rawlik, & Tenesa, 2017)), as well as supplementing this with additional studies identified
90 through Phenoscanner (Staley et al., 2016). We performed GWA for 249 proteins in two
91 European cohorts, and then adopted a proteome-by-phenome Mendelian randomisation
92 (P^2 MR) approach to assess the potential causal role of 64 proteins in 846 outcomes (e.g.
93 diseases, anthropomorphic measures, etc.). GeneAtlas results were further stratified
94 according to their consistency with a single underlying causal variant (affecting both
95 variation in protein concentration and outcome phenotype) or otherwise. Ultimately, of the

96 249 proteins, 38 were identified as causally contributing to human disease or other
97 quantitative trait.

98

99

Results

100 The abundance of an individual protein may be associated with DNA variants both local and
101 distant to its gene (termed local- and distal-pQTLs, respectively). We assayed the plasma
102 levels of 249 proteins using high-throughput, multiplex immunoassays and then performed
103 genome-wide association of these levels in two independent cohorts (discovery and
104 replication) of 909 and 998 European individuals. P²MR was applied to 54,144 exposure-
105 outcome pairs obtained from 64 significantly (p-value $<5 \times 10^{-8}$) associated, replicated
106 (Bonferroni correction for multiple testing), local-pQTLs, and 778 phenotypes obtained from
107 GeneAtlas (UK Biobank (Canela-Xandri et al., 2017)) and 68 phenotypes from 20 additional
108 genome-wide association (meta-analysis) studies (The CARDIoGRAMplusC4D Consortium et
109 al., 2015; R. A. Scott et al., 2017; C. P. Nelson et al., 2017; Liu et al., 2015; Schizophrenia
110 Working Group of the Psychiatric Genomics Consortium et al., 2014; Bronson et al., 2016;
111 Okada et al., 2014; van Rheenen et al., 2016; Hammerschlag et al., 2017; Sniekers et al., 2017;
112 Okbay et al., 2016; Hou et al., 2016; Beaumont et al., 2018; Phelan et al., 2017; van der Harst
113 & Verweij, 2018; Berg et al., 2016; de Moor et al., 2015; The EARly Genetics and Lifecourse
114 Epidemiology (EAGLE) Eczema Consortium et al., 2015; M. A. Ferreira et al., 2017; Astle et al.,
115 2016) identified through Phenoscanner (Staley et al., 2016) (Figure 1; Supplementary Table
116 S1; Methods).

117

118 In total, we identified 509 protein-outcome links for which there is evidence of a causal role
119 of the exposure (protein) on the outcome phenotype (trait).

120

121 **pQTLs.** pQTLs were highly concordant between the two cohorts (Supplementary Table S2).

122 Of the 209 independent pQTLs identified in the discovery cohort (p-value $<5 \times 10^{-8}$), 154 were
123 successfully replicated (Bonferroni correction for multiple testing; consistent direction of

124 effect). These represented pQTLs for 82 proteins, all but two encoded by autosomal genes.
125 Lead variants (smallest p-value within the locus; Methods) were identified at each locus, the
126 majority (64/80; 80%) of these proteins had the lead variant of one or more pQTLs located
127 close to the gene encoding the protein (± 150 kb; Figure 1) and hence were used as
128 instrumental variables suitable for MR. In many respects, locally-acting pQTLs are ideal
129 instrumental variables: they have large effect sizes, have highly plausible biological
130 relationships with protein level, and provide quantitative information about (often) directly
131 druggable protein targets. This is in contrast to distal pQTLs: the pathway through which
132 they exert their effects is generally unknown, with no *a priori* expectation of a direct effect on
133 a single target gene.

134

135 **Outcome GWA Studies.** Results linking the genetic variants and outcome traits and diseases
136 were obtained from secondary cohorts. UK Biobank has captured a wealth of information on
137 a large – approximately 500,000 individuals – population cohort that includes
138 anthropometry, haematological traits, and disease outcomes. Genome-wide association of
139 778 phenotypes from UK Biobank has been performed and published as GeneAtlas (Canela-
140 Xandri et al., 2017). Although the cohort is large, for many diseases the number of UK
141 Biobank individuals affected is small, resulting in low statistical power. Consequently, we
142 augmented these results with additional studies identified using Phenoscanner (Staley et al.,
143 2016) (Methods).

144

145 **Mendelian Randomisation.** MR depends upon an assumption that the DNA variant used as
146 an instrumental variable is robustly associated with the exposure. In our case we ensured
147 this by using stringent discovery and replication criteria for instrument selection. By limiting
148 ourselves to using locally-acting pQTLs as instruments, we sought to leverage *a priori*
149 biological knowledge regarding cellular protein production to substantially increase
150 confidence in the existence of a direct path from DNA variant to protein, and from protein to
151 outcome. P²MR yielded 271 protein-outcome pairs that were significant (false discovery rate
152 (FDR) <0.05) in UK Biobank, and 238 significant (FDR <0.05) pairs using data from

153 Phenoscanner. Thirty-two of the 64 proteins were causally implicated for one or more
154 outcomes in UK Biobank, and 36 of 64 in the outcomes identified through Phenoscanner
155 studies. The outcomes from GeneAtlas and Phenoscanner are not mutually exclusive, and
156 some of the studies included from Phenoscanner included data from UK Biobank, however,
157 overall, 38 of the 64 proteins (60%) were implicated in at least one outcome (Supplementary
158 Tables S3 and S4).

159

160 Proteins were implicated in diseases ranging from schizophrenia to cardiovascular disease
161 (Figure 2, Supplementary Tables S3 and S4). We applied a method, HEIDI (Zhu et al., 2016),
162 which explicitly accounts for the linkage disequilibrium (LD) structure of the locus to assess
163 the heterogeneity of MR effect estimates between the lead variant (the primary instrument)
164 and those of linked variants. HEIDI tests the hypothesis that the observed MR results are
165 caused by two distinct causal variants. Of the UK Biobank causal inferences, 77 survived the
166 HEIDI heterogeneity test (p-value >0.05). Therefore, these 77 proteins have (a) high-quality
167 evidence of association to a DNA variant which provides congruent predictions for both
168 plasma protein levels and disease risk / outcome phenotype, and (b) because of the physical
169 proximity to the SNP to the coding-sequence of the gene for the protein, and non-significant
170 HEIDI result, a low risk of pleiotropy (Supplementary Tables S3). These pairs thus provide
171 the most robust evidence that the level of the protein directly alters disease risk / outcome
172 phenotype.

173

174 However, all 509 causal inferences (271 from GeneAtlas (Canela-Xandri et al., 2017) and 238
175 from studies identified through Phenoscanner (Staley et al., 2016); Figures 2, S1, S2, S3, S4,
176 and Tables S3 and S4), even those consistent with heterogeneity, remain potential high
177 quality drug targets. This is because the HEIDI heterogeneity test (Figure 1) is susceptible to
178 type I errors in this context, as it does not account for multiple causal variants in a locus. In
179 addition, we apply HEIDI in a conservative manner: as a significant HEIDI test implies
180 heterogeneity, we did not apply a multiple testing correction. If a Bonferroni correction (271

181 tests) were to be applied to the HEIDI p-value, 180 of the protein-outcome pairs are not
182 significantly heterogeneous.

183

184 For some of these inferences, genetic evidence of an association between a protein and
185 phenotype has been proposed based on physical proximity of the genes to GWA intervals.
186 For nearly two-thirds (62%; 318/509) however, significant (FDR <0.05) MR association
187 between protein and outcome was not matched by significant (p-value <5x10⁻⁸) association
188 of the DNA variant to outcome. This suggests that P²MR has a greater potential to link
189 protein product and phenotype than naïve genome-wide association.

190

191 Our results draw causal inference between protein concentration and disease, for example,
192 IL4R and asthma, IL2RA and thyroid dysfunction, and IL12B and psoriasis (Figure 2). Taking
193 IL6R as an example, we found evidence for a causal association between plasma IL6R
194 abundance and coronary artery disease (CAD), atopy, and rheumatoid arthritis (Figure 2,
195 and Tables S3 and S4). We note that: 1) tocilizumab (an IL6 receptor antagonist) is in clinical
196 use for treating rheumatoid arthritis (L. J. Scott, 2017), 2) there is prior evidence from MR
197 demonstrating elevated levels of soluble IL6R and reduced cardiovascular disease (IL6R
198 Genetics Consortium Emerging Risk Factors Collaboration, 2012; Interleukin-6 Receptor
199 Mendelian Randomisation Analysis (IL6R MR) Consortium et al., 2012), and 3) the evidence
200 of a causal link between IL6R and atopy was not well established previously. Notably
201 however, tocilizumab has been used to treat three atopic dermatitis patients, and all patients
202 experienced >50% improvement in disease (Navarini, French, & Hofbauer, 2011). In
203 addition, Ullah et al. (2014) demonstrated that tocilizumab caused a reduction in Th2/Th17
204 response and associated airway inflammatory infiltration in a mouse model of experimental
205 allergic asthma.

206

207 As further illustration, we take two clinically important phenotypes as case-studies: CAD risk
208 and schizophrenia.

209

210 **CAD and FABP2:** P²MR identified 5 proteins as contributing to CAD pathogenesis: FABP2,
211 FGF5, IL6R, LPL, and LTA. Of these, 4 (FGF5, LPL, IL6R, and LTA) had been implicated
212 previously (Klarin et al., 2017; C. P. Nelson et al., 2017; Ozaki et al., 2002), whereas FABP2
213 had more limited evidence for its involvement.

214

215 FABP2 (intestinal fatty acid-binding protein) is causally linked by P²MR to CAD (Figure 2). A
216 FABP2 non-synonymous mutation (Ala54Thr) had been proposed as a risk factor for CAD
217 (Yuan, Yu, & Zeng, 2015), consistent with its P²MR candidature. However, of critical
218 importance to its potential utility as a therapeutic target, our study validates and extends this
219 association beyond the non-synonymous variant to protein abundance. pQTL analysis
220 identified two lead DNA variants in close proximity (<150kb) to the *FABP2* gene. Using the
221 SNP rs17009129, P²MR finds a causal link between FABP2 concentration and CAD ($p =$
222 1.1×10^{-4} ; FDR <0.05; $\beta_{MR} -0.11$; $se_{MR} 0.028$; β_{MR} and se_{MR} units: log(OR)/standard deviation of
223 residualised protein concentration) without significant heterogeneity ($p = 0.24$) which
224 suggests shared causal genetic control. Furthermore, a second independent SNP ($r^2 < 0.2$;
225 rs6857105) replicates this observation (MR $p = 5.0 \times 10^{-4}$; HEIDI $p = 0.34$; $\beta_{MR} -0.17$; se_{MR}
226 0.047). Both SNPs (rs17009129, and rs6857105) fell below genome-wide significance
227 ($p < 5 \times 10^{-8}$) in the full meta-analysis of van der Harst (van der Harst & Verweij, 2018) on
228 CAD; however, FABP2 was flagged as potentially relevant by DEPICT, a prioritization tool.
229 Consequently, this is the first time, to our knowledge, that variants associate with *FABP2*
230 concentration have been shown robustly to causally contribute to CAD pathogenesis.

231

232 **Schizophrenia:** By applying P²MR, we identified 3 proteins that were causally implicated in
233 the pathogenesis of schizophrenia: (i) Tyrosine-protein phosphatase non-receptor type
234 substrate 1 (SHPS1; *SIRPA*), (ii) Tumour necrosis factor receptor superfamily member 5
235 (*CD40*), and (iii) Low affinity immunoglobulin gamma Fc region receptor II-b (*FCGR2B*). The
236 link between SHPS1 (rs4813319) and schizophrenia risk was subsequently replicated in the
237 UK Biobank data (Methods; Table 1). The observed effect of SHSP1 on schizophrenia was not
238 significantly heterogeneous in the results of the Schizophrenia Working Group of the

239 Psychiatric Genomics Consortium (2014) ($p = 0.53$). Here we investigate *SHPS1* (approved
240 symbol *SIRPA*), which encodes SHPS1, tyrosine-protein phosphatase non-receptor type
241 substrate 1 and use *SHPS1* henceforth.

242

243 Interestingly, SHPS1 is highly expressed in the brain, especially in the neuropil (a dense
244 network of axons, dendrites, and microglial cell processes) in the cerebral cortex (“*SIRPA*
245 available from v18.proteinatlas.org,” 2018; “The Human Protein Atlas,” n.d.; Thul et al.,
246 2017; Uhlén et al., 2015; Uhlen et al., 2017), and co-localises with CD47 at dendrite-axon
247 contacts (Ohnishi et al., 2005). Mouse models in which the *SHPS1* gene is disrupted exhibit
248 many nervous system abnormalities, such as reduced long term potentiation, abnormal
249 synapse morphology and abnormal excitatory postsynaptic potential (MGI: 5558020
250 (“Mouse Genome Informatics (v6.13),” 2019; Toth et al., 2013)). Other mouse and rat models
251 link CD47 to sensorimotor gating and social behaviour phenotypes (H. P. Chang, Lindberg,
252 Wang, Huang, & Lee, 1999; Huang, Wang, Tang, & Lee, 1998; Koshimizu, Takao, Matozaki,
253 Ohnishi, & Miyakawa, 2014; Ma, Kuleskaya, Vöikar, & Tian, 2015; Ohnishi et al., 2010). In
254 addition, SHPS1 has been shown to mediate activity-dependent synapse maturation (Toth et
255 al., 2013) and may also have a role as a “don’t eat me” signal to microglia (Brown & Neher,
256 2014). Finally, SHPS1 levels tend to be lower in the dorsolateral prefrontal cortex of
257 schizophrenia patients (Martins-de-Souza et al., 2009).

258

259 **Table 1: Replication of significant Mendelian Randomisation (FDR <0.05) protein-to-**
260 **schizophrenia links in UK Biobank.**

261 Discovery: Mendelian randomisation p-value of protein level on schizophrenia risk, as
262 estimated using data from the Psychiatric Genomics Consortium – PGC (Schizophrenia
263 Working Group of the Psychiatric Genomics Consortium et al., 2014) obtained via
264 Phenoscanner (Staley et al., 2016).

265 Replication: The Mendelian Randomisation p-value of protein level on schizophrenia
266 (combined risk of 'F20-F29 Schizophrenia, schizotypal and delusional disorders' and self-
267 reported 'schizophrenia') in UK Biobank (Methods).

268 MR p-values are significant (FDR <0.05) in the Discovery sample.

269 † indicates significance of the replication study following multiple testing correction
270 (Bonferroni).

271

Gene	SNP	Discovery	Replication
<i>SHPS1</i>	rs4813319	1.1×10^{-3}	$5.3 \times 10^{-3\dagger}$
<i>FCGR2B</i>	rs4657041	1.0×10^{-3}	6.1×10^{-1}
<i>CD40</i>	rs4810485	1.5×10^{-3}	8.7×10^{-1}

272

273

Discussion

274 Proteome-by-phenome Mendelian Randomisation (P²MR) is an efficient method of
275 identifying potential drug targets through integrating pQTL with myriad phenotypes. P²MR
276 offers a data-driven approach to drug-discovery from population-level data. It quantifies the
277 strength of evidence for causation, together with magnitude and direction of effect, for
278 particular proteins in specific disease phenotypes. In addition, because MR using locally-
279 acting pQTLs is more focussed than a genome-wide study, the burden of multiple testing is
280 reduced dramatically, effectively reducing the sample-size required to declare a given effect
281 significant.

282

283 P²MR has some inherent limitations that need to be considered when interpreting results.
284 First, a true positive MR association in our analysis implies that any intervention to replicate
285 the effect of a given genotype would alter the relevant phenotype. Nevertheless, this
286 association is informative neither of the time interval, during development for example, nor
287 the anatomical location in which an intervention would need to be delivered. Second,
288 pleiotropic effects cannot be excluded entirely without (unachievable) quantification of
289 every mediator. Third, the concentration of a protein in plasma could be an imperfect proxy
290 for the effect of a drug targeting that protein at the level of a whole organism. Finally, plasma
291 concentration does not necessarily reflect activity. For example, a variant may cause
292 expression of high levels of an inactive form of a protein. Or, for proteins with both
293 membrane-bound and unbound forms, the MR direction of effect observed from quantifying
294 soluble protein abundance may not reflect that of membrane-bound protein. For many
295 membrane-bound proteins, a soluble (often antagonistic) form exists that is commonly
296 produced through alternative splicing or proteolytic cleavage of the membrane-bound form.
297 For example, tocilizumab, an IL6 receptor antagonist, is used as a treatment of rheumatoid
298 arthritis (L. J. Scott, 2017). The variant we use to instrument IL6R level, rs61812598, is in
299 complete LD with the missense variant rs2228145 in the British sub-population of 1,000
300 Genomes (Sudmant et al., 2015; The 1000 Genomes Project Consortium, 2015) whose effects
301 on proteolytic cleavage of the membrane-bound form and alternative splicing have been

302 examined in detail (R. C. Ferreira et al., 2013). Carriers of the 358Ala allele at rs2228145
303 tend to have increased soluble IL6R but reduced membrane-bound IL6R in a number of
304 immune cell types. Differences between the effects of soluble and membrane-bound forms of
305 a protein may be wide-spread. For example, Dupilumab is a monoclonal antibody that targets
306 IL4R, a key component of both IL4 and IL13 signalling. It is currently under investigation for
307 the treatment of asthma and has shown promising results in both eosinophilic and non-
308 eosinophilic asthma (Wenzel et al., 2016, 2013). Based on our results, we would have
309 predicted that increased levels of IL4R result in a lower risk of asthma (Supplementary Table
310 S3). This is in contrast to the direction-of-effect due to dupilumab administration. However,
311 as with IL6R, IL4R has both a soluble and a membrane-bound form. Encouragingly, despite
312 this, a relationship between dupilumab and asthma remains plausible – as evidenced by the
313 14 recently completed or ongoing clinical trials to assess the efficacy and safety of dupilumab
314 in asthma (As of 26 Mar 2019, ClinicalTrials.gov Identifiers: NCT01312961, NCT01854047,
315 NCT02134028, NCT02414854, NCT02528214, NCT02573233, NCT02948959,
316 NCT03112577, NCT03387852, NCT03560466, NCT03620747, NCT03694158,
317 NCT03782532, and NCT03884842).

318

319 P²MR provides an opportunity for studying the probable effects of specific proteins upon
320 human diseases, such as schizophrenia, for which only imperfect model systems currently
321 exist. Without a robust disease model, one must undertake studies in humans. However,
322 there is little justification to undertake an adequately powered randomised control trial of a
323 drug targeting a protein for which there is minimal evidence of a link between that protein
324 and disease. P²MR does not suffer from such limitations.

325

326 P²MR highlights FABP2 as contributory to the pathogenesis of CAD and there are orthogonal
327 lines of evidence to support this; notably: the non-synonymous mutation Ala54Thr (Yuan et
328 al., 2015). In addition, given its interaction with PPAR- α and fenofibrate (Hughes et al., 2015)
329 and strong expression in the gastrointestinal tract (“FABP2 available from

330 v18.proteinatlas.org,” 2018; “The Human Protein Atlas,” n.d.; Thul et al., 2017; Uhlén et al.,
331 2015; Uhlen et al., 2017), FABP2 represents a potential drug-target of the future.

332

333 Finally, as well as its utility in identifying potential therapeutic targets for drug development,
334 P²MR allows for an assessment of potential off-target effects of existing pharmacological
335 targets. For example, we predict an effect of IL4R modulation on eosinophil count and
336 percentage. This is an association already realised in one of the phase II clinical trials
337 investigating dupilumab in asthma: a rise in eosinophil count was observed for some
338 patients, even leading to the withdrawal of one patient from the study (Wenzel et al., 2016,
339 2013).

340

341

Conclusions

342 In summary, we have identified dozens of plausible causal links by conducting GWA of 249
343 proteins, followed by phenome-wide MR using replicated locally-acting pQTLs of 64
344 proteins: P²MR.

345 Using this approach, 54,144 protein-outcome links have been assessed and 509 significant
346 (FDR <0.05) links identified: including anthropometric measures, haematological
347 parameters, as well as diseases. Opportunities to discover larger sets of plausible causal links
348 will increase as study sizes and pQTL numbers grow. Indeed, whole-proteome versus
349 Biobank GWA Atlas studies will likely become feasible as pQTL measurement technologies
350 mature.

351

Methods

352 **Cohort description.** From the islands of Orkney (Scotland) and Vis (Croatia) respectively,
353 the ORCADES (McQuillan et al., 2008) and CROATIA-Vis (Campbell et al., 2007; Rudan et al.,
354 2009) studies are of two isolated population cohorts that are both genotyped and richly
355 phenotyped.

356 The Orkney Complex Disease Study (ORCADES) is a family-based, cross-sectional study that
357 seeks to identify genetic factors influencing cardiovascular and other disease risk in the
358 isolated archipelago of the Orkney Isles in northern Scotland (McQuillan et al., 2008). Genetic
359 diversity in this population is decreased compared to Mainland Scotland, consistent with the
360 high levels of endogamy historically. 2,078 participants aged 16-100 years were recruited
361 between 2005 and 2011, most having three or four grandparents from Orkney, the
362 remainder with two Orcadian grandparents. Fasting blood samples were collected and many
363 health-related phenotypes and environmental exposures were measured in each individual.
364 All participants gave written informed consent and the study was approved by Research
365 Ethics Committees in Orkney and Aberdeen (North of Scotland REC).

366 The CROATIA-Vis study includes 1,008 Croatians, aged 18-93 years, who were recruited
367 from the villages of Vis and Komiza on the Dalmatian island of Vis during spring of 2003 and
368 2004. All participants were volunteers and gave informed consent. They underwent a
369 medical examination and interview, led by research teams from the Institute for
370 Anthropological Research and the Andrija Stampar School of Public Health, (Zagreb, Croatia).
371 All subjects visited the clinical research centre in the region, where they were examined in
372 person and where fasting blood was drawn and stored for future analyses. Many biochemical
373 and physiological measurements were performed, and questionnaires of medical history as
374 well as lifestyle and environmental exposures were collected. The study received approval
375 from the relevant ethics committees in Scotland and Croatia (REC reference: 11/AL/0222)
376 and complied with the tenets of the Declaration of Helsinki.

377

378 **Genotyping.** Chromosomes and positions reported in this paper are from GRCh37
379 throughout. Genotyping of the ORCADES cohort was performed on the Illumina Human Hap
380 300v2, Illumina Omni Express, and Illumina Omni 1 arrays; that of the CROATIA-Vis cohort
381 used the Illumina HumanHap300v1 array.

382

383 The genotyping array data were subject to the following quality control thresholds: genotype
384 call-rate 0.98, per-individual call-rate 0.97, failed Hardy-Weinberg test at p-value $< 1 \times 10^{-6}$,

385 and minor allele frequency 0.01; genomic relationship matrix and principal components
386 were calculated using GenABEL (1.8-0) (Aulchenko, Ripke, Isaacs, & van Duijn, 2007) and
387 PLINK v1.90 (C. C. Chang et al., 2015; Purcell, 2017).

388

389 Assessment for ancestry outliers was performed by anchored PCA analysis when compared
390 to all non-European populations from the 1,000 Genomes project (Sudmant et al., 2015; The
391 1000 Genomes Project Consortium, 2015). Individuals with a mean-squared distance of
392 >10% in the first two principal components were removed. Genotypes were phased using
393 Shapeit v2.r873 and duoHMM (O'Connell et al., 2014) and imputed to the HRC.r1-1 reference
394 panel (The Haplotype Reference Consortium et al., 2016). 278,618 markers (Hap300) and
395 599,638 markers (Omni) were used for the imputation in ORCADES, and 272,930 markers
396 for CROATIA-Vis.

397

398 **Proteomics.** Plasma abundance of 249 proteins was measured in two European cohorts
399 using Olink Proseek Multiplex CVD2, CVD3, and INF panels. All proteomics measurements
400 were obtained from fasting EDTA plasma samples. Following quality control, there were 971
401 individuals in ORCADES, and 887 individuals in CROATIA-Vis, who had genotype and
402 proteomic data from Olink CVD2, 993 and 899 from Olink CVD3, and 982 and 894 from Olink
403 INF. The Olink Proseek Multiplex method uses a matched pair of antibodies for each protein,
404 linked to paired oligonucleotides. Binding of the antibodies to the protein brings the
405 oligonucleotides into close proximity and permits hybridization. Following binding and
406 extension, these oligonucleotides form the basis of a quantitative PCR reaction that allows
407 relative quantification of the initial protein concentration (Assarsson et al., 2014). Olink
408 panels include internal and external controls on each plate: two controls of the immunoassay
409 (two non-human proteins), one control of oligonucleotide extension (an antibody linked to
410 two matched oligonucleotides for immediate proximity, independent of antigen binding) and
411 one control of hybridized oligonucleotide detection (a pre-made synthetic double stranded
412 template), as well as an external, between-plate, control ("Olink," n.d.).

413

414 Prior to analysis, we excluded proteins with fewer than 200 samples with measurements
415 above the limit of detection of the assay. Of the 268 unique proteins reported by Olink, 253
416 passed this threshold in ORCADES, and 252 in CROATIA-Vis, with an intersect of 251
417 proteins. Protein values were inverse-normal rank-transformed prior to subsequent
418 analysis.

419

420 The subunits of IL27 are not distinguished in Olink's annotation (Q14213, *EBI3*; and
421 Q8NEV9, *IL27*). However, it has only one significant locus, local to the *EBI3* gene (lead
422 variant, rs60160662, is within 16kb). Therefore, *EBI3* (Q14213) was selected as
423 representative for this protein when discussing pQTL location (local/distal) so as to avoid
424 double counting.

425

426 Two proteins, CCL20 and BDNF, have been removed at the request of Olink.

427

428 **Genome-wide association of protein levels.** Genome-wide association of these proteins
429 was performed using autosomes only. Analyses were performed in three-stages. (1) a linear
430 regression model was used to account for participant age, sex, genotyping array (ORCADES
431 only), proteomics plate, proteomics plate row, proteomics plate column, length of sample
432 storage, season of venepuncture (ORCADES only), and the first 10 principal components of
433 the genomic relationship matrix. Genotyping array and season of venepuncture are invariant
434 in CROATIA-Vis and therefore were not included in the model. (2) Residuals from this model
435 were corrected for relatedness, using GenABELs (Aulchenko et al., 2007) polygenic function
436 and the genomic relationship matrix, to produce GRAMMAR+ residuals. Outlying
437 GRAMMAR+ residuals (absolute z-score >4) were removed and the remainder rank-based
438 inverse-normal transformed. (3) Genome-wide association testing was performed using
439 REGSCAN v0.5 (Haller, Kals, Esko, Magi, & Fischer, 2013).

440

441 **Reported pQTLs.** Genome-wide association results were clumped by linkage disequilibrium
442 using PLINK v1.90 (C. C. Chang et al., 2015; Purcell, 2017). Biallelic variants within $\pm 5\text{Mb}$ and

443 $r^2 > 0.2$ to the lead variant (smallest p-value at the locus) were clumped together, and the
444 lead variant is presented. r^2 was derived from all European populations in 1,000 Genomes
445 (Sudmant et al., 2015; The 1000 Genomes Project Consortium, 2015).

446

447 **Mendelian Randomisation.** In the context of P²MR, a DNA variant (a single nucleotide
448 polymorphism in this case) that influences plasma protein level is described as an
449 ‘instrumental variable’, the protein as the ‘exposure variable’, and the outcome phenotype as
450 the ‘outcome variable’.

451 A DNA variant was considered to be a potentially valid instrumental variable if it met the
452 following criteria:

- 453 (1) Minor allele frequency >1% in both ORCADES and CROATIA-Vis cohorts.
- 454 (2) An imputation info score (SNPTEST v2) of >0.95 in both ORCADES and CROATIA-Vis.
- 455 (3) Located within ±150kb of the gene coding for the protein (start and end coordinates
456 of the gene as defined by Ensembl GRCh37 (Zerbino et al., 2018)).

457

458 DNA variant selection was performed using the discovery (CROATIA-Vis) cohort. Replication
459 was defined based on a Bonferroni correction for the number of genome-wide significant
460 lead variants selected in the discovery cohort (CROATIA-Vis). In order to avoid a ‘winner’s
461 curse’, replicated genome-wide association effect sizes and standard errors from the
462 replication cohort (ORCADES) were used for MR.

463

464 We perform MR as a ratio of expectations, using up to second-order partial derivatives of the
465 Taylor series expansion for effect size estimates, and up to first-order for standard errors
466 (Delta method) (Lynch & Walsh, 1998):

467

468

469

470 (1)
$$\beta_{YX} \approx \frac{\beta_{YZ}}{\beta_{XZ}} \left(1 + \frac{se_{XZ}^2}{\beta_{XZ}^2} \right)$$

471 (2)
$$se_{YX} \approx \sqrt{\frac{se_{YZ}^2}{\beta_{XZ}^2} + \frac{\beta_{YZ}^2 \cdot se_{XZ}^2}{\beta_{XZ}^4}}$$

472 (3)
$$p_{YX} = 2\Phi(-|\beta_{YX}|/se_{YX})$$

473

474 where β_{ij} is the causal effect of j on i , se_{ij} is the standard error of the causal effect estimate of j
475 on i ; subscript X is the exposure, Y the outcome trait, and Z the instrumental variable. Φ is the
476 cumulative density function of the standard normal distribution.

477 **DNA variant to trait association: GeneAtlas.** All outcome GWA (778 traits) from GeneAtlas
478 (Canela-Xandri et al., 2017) were included. For each protein, the lead (lowest DNA variant-
479 protein association p-value in the discovery cohort) biallelic (Phase 3, 1,000 Genomes
480 (Sudmant et al., 2015; The 1000 Genomes Project Consortium, 2015)) variant meeting the
481 criteria above and an imputation info score >0.95 in UK Biobank, was selected for each
482 protein, and MR performed. An FDR of <0.05 was considered to be significant.

483 **DNA variant to trait association: PhenoScanner.** PhenoScanner (“PhenoScanner,” 2018;
484 Staley et al., 2016) was used to highlight existing GWA studies for inclusion. For each protein,
485 the lead (lowest DNA variant-protein association p-value in the discovery cohort) biallelic
486 (1,000 Genomes (Sudmant et al., 2015; The 1000 Genomes Project Consortium, 2015))
487 meeting the criteria above was selected. rs545634 was not found in the PhenoScanner
488 database and was therefore replaced with the second most significant variant meeting the
489 above criteria: chr1:15849003. PhenoScanner was run with the following options: Catalogue:
490 ‘Diseases & Traits’, p-value cut-off: ‘1’, Proxies: ‘None’, Build ‘37’. Results from 20 additional
491 studies were obtained, corresponding to 68 outcomes. The results from those studies that
492 returned a value for all input variants were kept and MR performed. An FDR of <0.05 was
493 considered to be significant.

494 **HEIDI.** heterogeneity in dependent instruments (HEIDI) analysis (Zhu et al., 2016), is a
495 method of testing whether the MR estimates obtained using variants in linkage
496 disequilibrium with the lead variant are consistent with a single causal variant or multiple

497 causal variant at a given locus (Figure 1D). HEIDI analysis was performed using software
498 provided at <https://cnsgenomics.com/software/smr/> [accessed 28/08/2018; v0.710]. We
499 created a bespoke BESD format file containing the pQTL data from ORCADES for assessment
500 as the exposure. Biallelic variants from the 1,000 Genomes (Sudmant et al., 2015; The 1000
501 Genomes Project Consortium, 2015) (European populations: CEU, FIN, GBR, IBS, and TSI)
502 were used as the linkage disequilibrium reference. We used the default 'cis-window' of
503 2000kb, and a maximum number of variants of 20 (as this is now the default value for the
504 software: based on unpublished power calculations by the authors of HEIDI and noted on
505 their website).

506

507 We performed HEIDI analysis of all exposure-outcome links that were found to be significant
508 (FDR <0.05) using outcomes from UK Biobank (n=271), as well as those links found to be MR
509 significant (FDR <0.05) with CAD from the meta-analysis of van der Harst (van der Harst &
510 Verweij, 2018), and for SHPS1 and schizophrenia (Schizophrenia Working Group of the
511 Psychiatric Genomics Consortium et al., 2014).

512

513 We applied the following filters for variants to be included in the analysis: minor allele
514 frequency MAF > 0.01 and, in the GeneAtlas and ORCADES data, an imputation info score of
515 >0.95.

516

517 **Schizophrenia GWA study replication.** In the initial analysis of Canela-Xandri et al. (2017),
518 schizophrenia was included as 'F20 Schizophrenia', and nested in 'F20-F29 Schizophrenia,
519 schizotypal and delusional disorders'. There were 920 cases in 'F20-F29 Schizophrenia,
520 schizotypal and delusional disorders' and 509 in 'F20 Schizophrenia'. Due to the near
521 doubling of the sample size, replication was attempted in the parent category: 'F20-F29
522 Schizophrenia, schizotypal and delusional disorders'. Using a Bonferroni correction, none of
523 these links replicated. However, due to the severe contraction of the number of cases present
524 in the sample – 35,476 cases and 46,839 controls to 920 cases and 407,535 controls – there
525 was a significant risk of false negative results. In order to address this, we re-analysed the UK

526 Biobank data including 'F20-F29 Schizophrenia, schizotypal and delusional disorders' and
527 self-reported 'schizophrenia' as a single outcome in a more permissive set of individuals:
528 individuals self-reporting their ethnicity as 'White' and clustering as a group based on the
529 first two genomic principal components (Canela-Xandri, Rawlik, & Tenesa, 2018). This
530 increased the number of cases and controls to 1,241 cases and 451,023 controls.

531

532

533

534

535

Acknowledgements

536 • A debt of gratitude is owed to all the participants in all cohorts used, without whom
537 this work would not have been possible.

538 • This research has been conducted using the UK Biobank Resource under project 788.

539 • Funding:

540 ○ ADB would like to acknowledge funding from the Wellcome PhD training
541 fellowship for clinicians (204979/Z/16/Z), the Edinburgh Clinical Academic
542 Track (ECAT) programme.

543 ○ TB, YZ, CA, PN, JFW, VV, CHay, CPP and CHal are supported by MRC University
544 Unit Programme Grants to the Human Genetics Unit (MC_PC_U127592696,
545 MC_UU_12008/1, MC_UU_00007/10 and MC_UU_00007/15)

546 ○ AT, OC-X and KR acknowledge funding from the MRC (MR/R025851/1,
547 MR/N003179/1).

548 ○ CHal, JKB, AT, and KR acknowledge funding from BBSRC Institute
549 Strategic Programme grants to the Roslin Institute
550 (BBS/E/D/30002275, BBS/E/D/30002276, BBS/E/D/10002071,
551 BBS/E/D/20002172, BBS/E/D/20002174).

552 ○ PKJ would like to acknowledge funding from the Axa research fund.

- 553 ○ JKB acknowledges funding support from a Wellcome-Beit Prize
554 Intermediate Clinical Fellowship (103258/Z/13/Z,A), and the UK
555 Intensive Care Foundation.
- 556
- 557 • The Orkney Complex Disease Study (ORCADES) was supported by the Chief Scientist
558 Office of the Scottish Government (CZB/4/276, CZB/4/710), a Royal Society URF to
559 JFW, the MRC Human Genetics Unit quinquennial programme “QTL in Health and
560 Disease”, Arthritis Research UK and the European Union framework program 6
561 EUROSPAN project (contract no. LSHG-CT-2006-018947). DNA extractions were
562 performed at the Wellcome Trust Clinical Research Facility in Edinburgh. We would
563 like to acknowledge the invaluable contributions of the research nurses in Orkney, the
564 administrative team in Edinburgh and the people of Orkney.
- 565 • The CROATIA-Vis study was funded by grants from the Medical Research Council (UK)
566 and Republic of Croatia Ministry of Science, Education and Sports research grants.
567 (108-1080315-0302). We would like to acknowledge the staff of several institutions in
568 Croatia that supported the field work, including but not limited to The University of
569 Split and Zagreb Medical Schools, the Institute for Anthropological Research in Zagreb
570 and Croatian Institute for Public Health. Genotyping was performed in the Genetics
571 Core of the Clinical Research Facility, University of Edinburgh.

572

573

References

- 574 Arrowsmith, J. (2011). Trial watch: Phase II failures: 2008-2010. *Nature Reviews*
575 *Drug Discovery*, 10, 328–329. <https://doi.org/10.1038/nrd3439>
- 576 Assarsson, E., Lundberg, M., Holmquist, G., Björkesten, J., Bucht Thorsen, S., Ekman,
577 D., ... Fredriksson, S. (2014). Homogenous 96-Plex PEA Immunoassay
578 Exhibiting High Sensitivity, Specificity, and Excellent Scalability. *PLOS ONE*,
579 9(4), e95192. <https://doi.org/10.1371/journal.pone.0095192>
- 580 Astle, W. J., Elding, H., Jiang, T., Allen, D., Ruklisa, D., Mann, A. L., ... Soranzo, N.
581 (2016). The Allelic Landscape of Human Blood Cell Trait Variation and

- 582 Links to Common Complex Disease. *Cell*, 167(5), 1415-1429.e19.
583 <https://doi.org/10.1016/j.cell.2016.10.042>
- 584 Aulchenko, Y. S., Ripke, S., Isaacs, A., & van Duijn, C. M. (2007). GenABEL: an R
585 library for genome-wide association analysis. *Bioinformatics (Oxford,*
586 *England)*, 23(10), 1294-1296.
587 <https://doi.org/10.1093/bioinformatics/btm108>
- 588 Baillie, J. K. (2014). Translational genomics. Targeting the host immune response to
589 fight infection. *Science (New York, N.Y.)*, 344(6186), 807-808.
590 <https://doi.org/10.1126/science.1255074>
- 591 Baillie, J. K., Bretherick, A., Haley, C. S., Clohisey, S., Gray, A., Neyton, L. P. A., ... Hume,
592 D. A. (2018). Shared activity patterns arising at genetic susceptibility loci
593 reveal underlying genomic and cellular architecture of human disease. *PLoS*
594 *Computational Biology*, 14(3), e1005934.
595 <https://doi.org/10.1371/journal.pcbi.1005934>
- 596 Beaumont, R. N., Warrington, N. M., Cavadino, A., Tyrrell, J., Nodzinski, M.,
597 Horikoshi, M., ... Freathy, R. M. (2018). Genome-wide association study of
598 offspring birth weight in 86 577 women identifies five novel loci and
599 highlights maternal genetic effects that are independent of fetal genetics.
600 *Human Molecular Genetics*, 27(4), 742-756.
601 <https://doi.org/10.1093/hmg/ddx429>
- 602 Berg, S. M. van den, Moor, M. H. M. de, Verweij, K. J. H., Krueger, R. F., Luciano, M.,
603 Vasquez, A. A., ... Boomsma, D. I. (2016). Meta-analysis of Genome-Wide
604 Association Studies for Extraversion: Findings from the Genetics of
605 Personality Consortium. *Behavior Genetics*, 46(2), 170-182.
606 <https://doi.org/10.1007/s10519-015-9735-5>
- 607 Bronson, P. G., Chang, D., Bhangale, T., Seldin, M. F., Ortmann, W., Ferreira, R. C., ...
608 Behrens, T. W. (2016). Common variants at PVT1, ATG13-AMBRA1, AHI1
609 and CLEC16A are associated with selective IgA deficiency. *Nature Genetics*,
610 48(11), 1425-1429. <https://doi.org/10.1038/ng.3675>

- 611 Brown, G. C., & Neher, J. J. (2014). Microglial phagocytosis of live neurons. *Nature*
612 *Reviews Neuroscience*, *15*(4), 209–216. <https://doi.org/10.1038/nrn3710>
- 613 Campbell, H., Carothers, A. D., Rudan, I., Hayward, C., Biloglav, Z., Barac, L., ... Wright,
614 A. F. (2007). Effects of genome-wide heterozygosity on a range of
615 biomedically relevant human quantitative traits. *Human Molecular Genetics*,
616 *16*(2), 233–241. <https://doi.org/10.1093/hmg/ddl473>
- 617 Canela-Xandri, O., Rawlik, K., & Tenesa, A. (2017). An atlas of genetic associations in
618 UK Biobank. *BioRxiv*, 176834. <https://doi.org/10.1101/176834>
- 619 Canela-Xandri, O., Rawlik, K., & Tenesa, A. (2018). An atlas of genetic associations in
620 UK Biobank. *Nature Genetics*, *50*(11), 1593.
621 <https://doi.org/10.1038/s41588-018-0248-z>
- 622 Chang, C. C., Chow, C. C., Tellier, L. C., Vattikuti, S., Purcell, S. M., & Lee, J. J. (2015).
623 Second-generation PLINK: rising to the challenge of larger and richer
624 datasets. *GigaScience*, *4*(1), 1–16. [https://doi.org/10.1186/s13742-015-](https://doi.org/10.1186/s13742-015-0047-8)
625 [0047-8](https://doi.org/10.1186/s13742-015-0047-8)
- 626 Chang, H. P., Lindberg, F. P., Wang, H. L., Huang, A. M., & Lee, E. H. Y. (1999).
627 Impaired Memory Retention and Decreased Long-Term Potentiation in
628 Integrin-Associated Protein-Deficient Mice. *Learning & Memory*, *6*(5), 448–
629 457.
- 630 Civelek, M., & Lusk, A. J. (2014). Systems genetics approaches to understand
631 complex traits. *Nature Reviews Genetics*, *15*(1), 34–48.
632 <https://doi.org/10.1038/nrg3575>
- 633 de Moor, M. H. M., van den Berg, S. M., Verweij, K. J. H., Krueger, R. F., Luciano, M.,
634 Arias Vasquez, A., ... Boomsma, D. I. (2015). Meta-analysis of Genome-wide
635 Association Studies for Neuroticism, and the Polygenic Association With
636 Major Depressive Disorder. *JAMA Psychiatry*, *72*(7), 642.
637 <https://doi.org/10.1001/jamapsychiatry.2015.0554>

638 FABP2 available from v18.proteinatlas.org. (2018, November 15). Retrieved April 1,
639 2019, from The Human Protein Atlas website:
640 <https://v18.proteinatlas.org/ENSG00000145384-FABP2/tissue>

641 Ferreira, M. A., Vonk, J. M., Baurecht, H., Marenholz, I., Tian, C., Hoffman, J. D., ...
642 Paternoster, L. (2017). Shared genetic origin of asthma, hay fever and
643 eczema elucidates allergic disease biology. *Nature Genetics*, 49(12), 1752–
644 1757. <https://doi.org/10.1038/ng.3985>

645 Ferreira, R. C., Freitag, D. F., Cutler, A. J., Howson, J. M. M., Rainbow, D. B., Smyth, D. J.,
646 ... Todd, J. A. (2013). Functional IL6R 358Ala Allele Impairs Classical IL-6
647 Receptor Signaling and Influences Risk of Diverse Inflammatory Diseases.
648 *PLOS Genetics*, 9(4), e1003444.
649 <https://doi.org/10.1371/journal.pgen.1003444>

650 Finan, C., Gaulton, A., Kruger, F. A., Lumbers, R. T., Shah, T., Engmann, J., ... Casas, J. P.
651 (2017). The druggable genome and support for target identification and
652 validation in drug development. *Science Translational Medicine*, 9(383),
653 eaag1166. <https://doi.org/10.1126/scitranslmed.aag1166>

654 Folkersen, L., Fauman, E., Sabater-Lleal, M., Strawbridge, R. J., Frånberg, M.,
655 Sennblad, B., ... Mälarstig, A. (2017). Mapping of 79 loci for 83 plasma
656 protein biomarkers in cardiovascular disease. *PLOS Genetics*, 13(4),
657 e1006706. <https://doi.org/10.1371/journal.pgen.1006706>

658 Haller, T., Kals, M., Esko, T., Magi, R., & Fischer, K. (2013). RegScan: a GWAS tool for
659 quick estimation of allele effects on continuous traits and their
660 combinations. *Briefings in Bioinformatics*, 16(1), 39–44.
661 <https://doi.org/10.1093/bib/bbt066>

662 Hammerschlag, A. R., Stringer, S., de Leeuw, C. A., Sniekers, S., Taskesen, E.,
663 Watanabe, K., ... Posthuma, D. (2017). Genome-wide association analysis of
664 insomnia complaints identifies risk genes and genetic overlap with
665 psychiatric and metabolic traits. *Nature Genetics*, 49(11), 1584–1592.
666 <https://doi.org/10.1038/ng.3888>

- 667 Hou, L., Bergen, S. E., Akula, N., Song, J., Hultman, C. M., Landén, M., ... McMahon, F. J.
668 (2016). Genome-wide association study of 40,000 individuals identifies two
669 novel loci associated with bipolar disorder. *Human Molecular Genetics*,
670 25(15), 3383–3394. <https://doi.org/10.1093/hmg/ddw181>
- 671 Huang, A.-M., Wang, H. L., Tang, Y. P., & Lee, E. H. Y. (1998). Expression of Integrin-
672 Associated Protein Gene Associated with Memory Formation in Rats.
673 *Journal of Neuroscience*, 18(11), 4305–4313.
- 674 Hughes, M. L. R., Liu, B., Halls, M. L., Wagstaff, K. M., Patil, R., Velkov, T., ... Porter, C. J.
675 H. (2015). Fatty Acid-binding Proteins 1 and 2 Differentially Modulate the
676 Activation of Peroxisome Proliferator-activated Receptor α in a Ligand-
677 selective Manner. *The Journal of Biological Chemistry*, 290(22), 13895–
678 13906. <https://doi.org/10.1074/jbc.M114.605998>
- 679 IL6R Genetics Consortium Emerging Risk Factors Collaboration. (2012).
680 Interleukin-6 receptor pathways in coronary heart disease: a collaborative
681 meta-analysis of 82 studies. *The Lancet*, 379(9822), 1205–1213.
682 [https://doi.org/10.1016/S0140-6736\(11\)61931-4](https://doi.org/10.1016/S0140-6736(11)61931-4)
- 683 Interleukin-6 Receptor Mendelian Randomisation Analysis (IL6R MR) Consortium,
684 Swerdlow, D. I., Holmes, M. V., Kuchenbaecker, K. B., Engmann, J. E. L., Shah,
685 T., ... Casas, J. P. (2012). The interleukin-6 receptor as a target for
686 prevention of coronary heart disease: a mendelian randomisation analysis.
687 *Lancet (London, England)*, 379(9822), 1214–1224.
688 [https://doi.org/10.1016/S0140-6736\(12\)60110-X](https://doi.org/10.1016/S0140-6736(12)60110-X)
- 689 Klarin, D., Zhu, Q. M., Emdin, C. A., Chaffin, M., Horner, S., McMillan, B. J., ...
690 Kathiresan, S. (2017). Genetic Analysis in UK Biobank Links Insulin
691 Resistance and Transendothelial Migration Pathways to Coronary Artery
692 Disease. *Nature Genetics*, 49(9), 1392–1397.
693 <https://doi.org/10.1038/ng.3914>
- 694 Koshimizu, H., Takao, K., Matozaki, T., Ohnishi, H., & Miyakawa, T. (2014).
695 Comprehensive Behavioral Analysis of Cluster of Differentiation 47

- 696 Knockout Mice. *PLOS ONE*, 9(2), e89584.
697 <https://doi.org/10.1371/journal.pone.0089584>
- 698 Liu, J. Z., van Sommeren, S., Huang, H., Ng, S. C., Alberts, R., Takahashi, A., ...
699 Weersma, R. K. (2015). Association analyses identify 38 susceptibility loci
700 for inflammatory bowel disease and highlight shared genetic risk across
701 populations. *Nature Genetics*, 47(9), 979–986.
702 <https://doi.org/10.1038/ng.3359>
- 703 Lynch, M., & Walsh, B. (1998). *Genetics and Analysis of Quantitative Traits* (1998
704 edition). Sunderland, Mass: Sinauer.
- 705 Ma, L., Kuleskaya, N., Vöikar, V., & Tian, L. (2015). Differential expression of brain
706 immune genes and schizophrenia-related behavior in C57BL/6N and
707 DBA/2J female mice. *Psychiatry Research*, 226(1), 211–216.
708 <https://doi.org/10.1016/j.psychres.2015.01.001>
- 709 MacArthur, J., Bowler, E., Cerezo, M., Gil, L., Hall, P., Hastings, E., ... Parkinson, H.
710 (2017). The new NHGRI-EBI Catalog of published genome-wide association
711 studies (GWAS Catalog). *Nucleic Acids Research*, 45(Database issue), D896–
712 D901. <https://doi.org/10.1093/nar/gkw1133>
- 713 Martins-de-Souza, D., Gattaz, W. F., Schmitt, A., Rewerts, C., Maccarrone, G., Dias-
714 Neto, E., & Turck, C. W. (2009). Prefrontal cortex shotgun proteome
715 analysis reveals altered calcium homeostasis and immune system
716 imbalance in schizophrenia. *European Archives of Psychiatry and Clinical
717 Neuroscience*, 259(3), 151–163. [https://doi.org/10.1007/s00406-008-
718 0847-2](https://doi.org/10.1007/s00406-008-0847-2)
- 719 McQuillan, R., Leutenegger, A.-L., Abdel-Rahman, R., Franklin, C. S., Pericic, M., Barac-
720 Lauc, L., ... Wilson, J. F. (2008). Runs of homozygosity in European
721 populations. *American Journal of Human Genetics*, 83(3), 359–372.
722 <https://doi.org/10.1016/j.ajhg.2008.08.007>

- 723 Mirauta, B., Seaton, D. D., Bensaddek, D., Brenes, A., Bonder, M. J., Kilpinen, H., ...
724 Lamond, A. (2018). Population-scale proteome variation in human induced
725 pluripotent stem cells. *BioRxiv*, 439216. <https://doi.org/10.1101/439216>
726 Mouse Genome Informatics (v6.13). (2019, March 26). Retrieved April 1, 2019, from
727 <http://www.informatics.jax.org/>
- 728 Munos, B. (2009). Lessons from 60 years of pharmaceutical innovation. *Nature*
729 *Reviews. Drug Discovery*, 8(12), 959–968.
730 <https://doi.org/10.1038/nrd2961>
- 731 Navarini, A. A., French, L. E., & Hofbauer, G. F. L. (2011). Interrupting IL-6–receptor
732 signaling improves atopic dermatitis but associates with bacterial
733 superinfection. *Journal of Allergy and Clinical Immunology*, 128(5), 1128–
734 1130. <https://doi.org/10.1016/j.jaci.2011.09.009>
- 735 Nelson, C. P., Goel, A., Butterworth, A. S., Kanoni, S., Webb, T. R., Marouli, E., ...
736 Deloukas, P. (2017). Association analyses based on false discovery rate
737 implicate new loci for coronary artery disease. *Nature Genetics*, 49(9),
738 1385–1391. <https://doi.org/10.1038/ng.3913>
- 739 Nelson, M. R., Tipney, H., Painter, J. L., Shen, J., Nicoletti, P., Shen, Y., ... Sansseau, P.
740 (2015). The support of human genetic evidence for approved drug
741 indications. *Nature Genetics*, 47(8), 856–860.
742 <https://doi.org/10.1038/ng.3314>
- 743 O’Connell, J., Gurdasani, D., Delaneau, O., Pirastu, N., Ulivi, S., Cocca, M., ... Marchini, J.
744 (2014). A General Approach for Haplotype Phasing across the Full
745 Spectrum of Relatedness. *PLOS Genetics*, 10(4), e1004234.
746 <https://doi.org/10.1371/journal.pgen.1004234>
- 747 Ohnishi, H., Kaneko, Y., Okazawa, H., Miyashita, M., Sato, R., Hayashi, A., ... Matozaki,
748 T. (2005). Differential Localization of Src Homology 2 Domain-Containing
749 Protein Tyrosine Phosphatase Substrate-1 and CD47 and Its Molecular
750 Mechanisms in Cultured Hippocampal Neurons. *Journal of Neuroscience*,
751 25(10), 2702–2711. <https://doi.org/10.1523/JNEUROSCI.5173-04.2005>

- 752 Ohnishi, H., Murata, T., Kusakari, S., Hayashi, Y., Takao, K., Maruyama, T., ... Matozaki,
753 T. (2010). Stress-Evoked Tyrosine Phosphorylation of Signal Regulatory
754 Protein α Regulates Behavioral Immobility in the Forced Swim Test. *Journal*
755 *of Neuroscience*, 30(31), 10472–10483.
756 <https://doi.org/10.1523/JNEUROSCI.0257-10.2010>
- 757 Okada, Y., Wu, D., Trynka, G., Raj, T., Terao, C., Ikari, K., ... Plenge, R. M. (2014).
758 Genetics of rheumatoid arthritis contributes to biology and drug discovery.
759 *Nature*, 506(7488), 376–381. <https://doi.org/10.1038/nature12873>
- 760 Okbay, A., Beauchamp, J. P., Fontana, M. A., Lee, J. J., Pers, T. H., Rietveld, C. A., ...
761 Benjamin, D. J. (2016). Genome-wide association study identifies 74 loci
762 associated with educational attainment. *Nature*, 533(7604), 539–542.
763 <https://doi.org/10.1038/nature17671>
- 764 Olink. (n.d.). Retrieved June 19, 2016, from <http://www.olink.com/>
- 765 Ozaki, K., Ohnishi, Y., Iida, A., Sekine, A., Yamada, R., Tsunoda, T., ... Tanaka, T.
766 (2002). Functional SNPs in the lymphotoxin-alpha gene that are associated
767 with susceptibility to myocardial infarction. *Nature Genetics*, 32(4), 650–
768 654. <https://doi.org/10.1038/ng1047>
- 769 Phelan, C. M., Kuchenbaecker, K. B., Tyrer, J. P., Kar, S. P., Lawrenson, K., Winham, S.
770 J., ... Pharoah, P. D. P. (2017). Identification of 12 new susceptibility loci for
771 different histotypes of epithelial ovarian cancer. *Nature Genetics*, 49(5),
772 680–691. <https://doi.org/10.1038/ng.3826>
- 773 PhenoScanner. (2018). Retrieved September 25, 2018, from
774 <http://www.phenoscaner.medschl.cam.ac.uk/>
- 775 Pruim, R. J., Welch, R. P., Sanna, S., Teslovich, T. M., Chines, P. S., Gliedt, T. P., ...
776 Willer, C. J. (2010). LocusZoom: regional visualization of genome-wide
777 association scan results. *Bioinformatics (Oxford, England)*, 26(18), 2336–
778 2337. <https://doi.org/10.1093/bioinformatics/btq419>
- 779 Purcell, S. (2017). PLINK: v1.90b3.46 (Version v1.90).

- 780 Rudan, I., Marusić, A., Janković, S., Rotim, K., Boban, M., Lauc, G., ... Polasek, O.
781 (2009). "10001 Dalmatians:" Croatia launches its national biobank.
782 *Croatian Medical Journal*, 50(1), 4–6.
- 783 Schizophrenia Working Group of the Psychiatric Genomics Consortium, Ripke, S.,
784 Neale, B. M., Corvin, A., Walters, J. T. R., Farh, K.-H., ... O'Donovan, M. C.
785 (2014). Biological insights from 108 schizophrenia-associated genetic loci.
786 *Nature*, 511(7510), 421–427. <https://doi.org/10.1038/nature13595>
- 787 Scott, L. J. (2017). Tocilizumab: A Review in Rheumatoid Arthritis. *Drugs*, 77(17),
788 1865–1879. <https://doi.org/10.1007/s40265-017-0829-7>
- 789 Scott, R. A., Scott, L. J., Mägi, R., Marullo, L., Gaulton, K. J., Kaakinen, M., ... DIAbetes
790 Genetics Replication And Meta-analysis (DIAGRAM) Consortium. (2017).
791 An Expanded Genome-Wide Association Study of Type 2 Diabetes in
792 Europeans. *Diabetes*, 66(11), 2888–2902. [https://doi.org/10.2337/db16-](https://doi.org/10.2337/db16-1253)
793 1253
- 794 SIRPA available from v18.proteinatlas.org. (2018, November 15). Retrieved April 1,
795 2019, from The Human Protein Atlas website:
796 <https://v18.proteinatlas.org/ENSG00000198053-SIRPA/tissue>
- 797 Smith, G. D., & Ebrahim, S. (2003). "Mendelian randomization": can genetic
798 epidemiology contribute to understanding environmental determinants of
799 disease? *International Journal of Epidemiology*, 32(1), 1–22.
- 800 Sniekers, S., Stringer, S., Watanabe, K., Jansen, P. R., Coleman, J. R. I., Krapohl, E., ...
801 Posthuma, D. (2017). Genome-wide association meta-analysis of 78,308
802 individuals identifies new loci and genes influencing human intelligence.
803 *Nature Genetics*, 49(7), 1107–1112. <https://doi.org/10.1038/ng.3869>
- 804 Staley, J. R., Blackshaw, J., Kamat, M. A., Ellis, S., Surendran, P., Sun, B. B., ...
805 Butterworth, A. S. (2016). PhenoScanner: a database of human genotype–
806 phenotype associations. *Bioinformatics*, 32(20), 3207–3209.
807 <https://doi.org/10.1093/bioinformatics/btw373>

808 Sudmant, P. H., Rausch, T., Gardner, E. J., Handsaker, R. E., Abyzov, A., Huddleston, J.,
809 ... Korbel, J. O. (2015). An integrated map of structural variation in 2,504
810 human genomes. *Nature*, 526(7571), 75–81.
811 <https://doi.org/10.1038/nature15394>

812 Suhre, K., Arnold, M., Bhagwat, A. M., Cotton, R. J., Engelke, R., Raffler, J., ...
813 Graumann, J. (2017). Connecting genetic risk to disease end points through
814 the human blood plasma proteome. *Nature Communications*, 8, 14357.
815 <https://doi.org/10.1038/ncomms14357>

816 Sun, B. B., Maranville, J. C., Peters, J. E., Stacey, D., Staley, J. R., Blackshaw, J., ...
817 Butterworth, A. S. (2018). Genomic atlas of the human plasma proteome.
818 *Nature*, 558(7708), 73. <https://doi.org/10.1038/s41586-018-0175-2>

819 The 1000 Genomes Project Consortium. (2015). A global reference for human
820 genetic variation. *Nature*, 526(7571), 68–74.
821 <https://doi.org/10.1038/nature15393>

822 The CARDIoGRAMplusC4D Consortium, Nikpay, M., Goel, A., Won, H.-H., Hall, L. M.,
823 Willenborg, C., ... Farrall, M. (2015). A comprehensive 1000 Genomes-
824 based genome-wide association meta-analysis of coronary artery disease.
825 *Nature Genetics*, 47(10), 1121–1130. <https://doi.org/10.1038/ng.3396>

826 The EARly Genetics and Lifecourse Epidemiology (EAGLE) Eczema Consortium,
827 Paternoster, L., Standl, M., Waage, J., Baurecht, H., Hotze, M., ... Weidinger, S.
828 (2015). Multi-ancestry genome-wide association study of 21,000 cases and
829 95,000 controls identifies new risk loci for atopic dermatitis. *Nature*
830 *Genetics*, 47(12), 1449–1456. <https://doi.org/10.1038/ng.3424>

831 The Haplotype Reference Consortium, McCarthy, S., Das, S., Kretzschmar, W.,
832 Delaneau, O., Wood, A. R., ... Marchini, J. (2016). A reference panel of 64,976
833 haplotypes for genotype imputation. *Nature Genetics*, 48(10), 1279–1283.
834 <https://doi.org/10.1038/ng.3643>

835 The Human Protein Atlas. (n.d.). Retrieved December 13, 2017, from
836 <https://www.proteinatlas.org/>

- 837 Thul, P. J., Åkesson, L., Wiking, M., Mahdessian, D., Geladaki, A., Blal, H. A., ...
838 Lundberg, E. (2017). A subcellular map of the human proteome. *Science*,
839 356(6340), eaal3321. <https://doi.org/10.1126/science.aal3321>
- 840 Toth, A. B., Terauchi, A., Zhang, L. Y., Johnson-Venkatesh, E. M., Larsen, D. J., Sutton,
841 M. A., & Umemori, H. (2013). Synapse maturation by activity-dependent
842 ectodomain shedding of SIRP α . *Nature Neuroscience*, 16(10), 1417.
843 <https://doi.org/10.1038/nn.3516>
- 844 Uhlén, M., Fagerberg, L., Hallström, B. M., Lindskog, C., Oksvold, P., Mardinoglu, A., ...
845 Pontén, F. (2015). Tissue-based map of the human proteome. *Science*,
846 347(6220), 1260419. <https://doi.org/10.1126/science.1260419>
- 847 Uhlen, M., Zhang, C., Lee, S., Sjöstedt, E., Fagerberg, L., Bidkhor, G., ... Ponten, F.
848 (2017). A pathology atlas of the human cancer transcriptome. *Science*,
849 357(6352), eaan2507. <https://doi.org/10.1126/science.aan2507>
- 850 Ullah, M. A., Sukkar, M., Ferreira, M., & Phipps, S. (2014). 53: IL-6R blockade: A new
851 personalised treatment for asthma? *Cytokine*, 70(1), 40.
852 <https://doi.org/10.1016/j.cyto.2014.07.060>
- 853 van der Harst, P., & Verweij, N. (2018). Identification of 64 Novel Genetic Loci
854 Provides an Expanded View on the Genetic Architecture of Coronary Artery
855 Disease. *Circulation Research*, 122(3), 433–443.
856 <https://doi.org/10.1161/CIRCRESAHA.117.312086>
- 857 van Rheenen, W., Shatunov, A., Dekker, A. M., McLaughlin, R. L., Diekstra, F. P., Pulit,
858 S. L., ... Veldink, J. H. (2016). Genome-wide association analyses identify
859 new risk variants and the genetic architecture of amyotrophic lateral
860 sclerosis. *Nature Genetics*, 48(9), 1043–1048.
861 <https://doi.org/10.1038/ng.3622>
- 862 Wenzel, S., Castro, M., Corren, J., Maspero, J., Wang, L., Zhang, B., ... Teper, A. (2016).
863 Dupilumab efficacy and safety in adults with uncontrolled persistent
864 asthma despite use of medium-to-high-dose inhaled corticosteroids plus a
865 long-acting β 2 agonist: a randomised double-blind placebo-controlled

866 pivotal phase 2b dose-ranging trial. *The Lancet*, 388(10039), 31–44.
867 [https://doi.org/10.1016/S0140-6736\(16\)30307-5](https://doi.org/10.1016/S0140-6736(16)30307-5)

868 Wenzel, S., Ford, L., Pearlman, D., Spector, S., Sher, L., Skobieranda, F., ... Pirozzi, G.
869 (2013). Dupilumab in Persistent Asthma with Elevated Eosinophil Levels.
870 *New England Journal of Medicine*, 368(26), 2455–2466.
871 <https://doi.org/10.1056/NEJMoa1304048>

872 Yao, C., Chen, G., Song, C., Keefe, J., Mendelson, M., Huan, T., ... Levy, D. (2018).
873 Genome-wide mapping of plasma protein QTLs identifies putatively causal
874 genes and pathways for cardiovascular disease. *Nature Communications*,
875 9(1), 3268. <https://doi.org/10.1038/s41467-018-05512-x>

876 Yuan, D., Yu, C., & Zeng, C. (2015). Association of I-FABP gene polymorphism and the
877 risk of coronary heart disease. *International Journal of Clinical and*
878 *Experimental Medicine*, 8(9), 16389–16393.

879 Zerbino, D. R., Achuthan, P., Akanni, W., Amode, M. R., Barrell, D., Bhai, J., ... Flicek, P.
880 (2018). Ensembl 2018. *Nucleic Acids Research*, 46(D1), D754–D761.
881 <https://doi.org/10.1093/nar/gkx1098>

882 Zhu, Z., Zhang, F., Hu, H., Bakshi, A., Robinson, M. R., Powell, J. E., ... Yang, J. (2016).
883 Integration of summary data from GWAS and eQTL studies predicts
884 complex trait gene targets. *Nature Genetics*, 48(5), 481–487.
885 <https://doi.org/10.1038/ng.3538>

886

887

Supplementary Materials

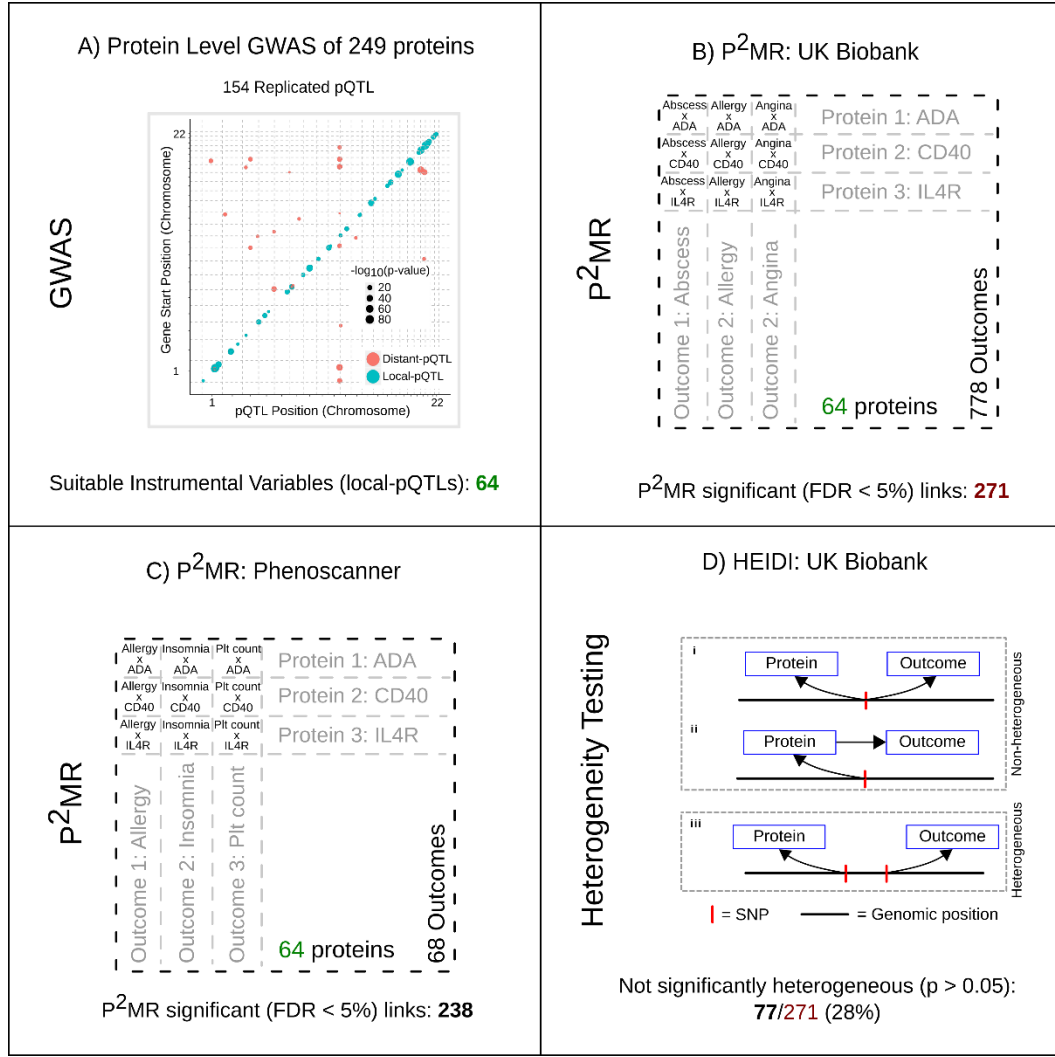
- 888 • Table S1. Additional studies identified using Phenoscanner: additional_studies.tsv.
- 889 • Table S2. Complete list of pQTLs (linkage disequilibrium clumped): indep_pqtl.tsv.
- 890 • Table S3. Mendelian Randomisation results from UK Biobank: df_ukbb_heidi.tsv.
- 891 • Table S4. Mendelian Randomisation results from studies identified using
892 Phenoscanner: df_phenoscanner.tsv.
- 893 • Figure S1. Significant (FDR <0.05) P2MR protein-outcome causal inferences:
894 haematology count subset.
- 895 • Figure S2. Significant (FDR <0.05) P2MR protein-outcome causal inferences:
896 haematology percentage subset.
- 897 • Figure S3. Significant (FDR <0.05) P2MR protein-outcome causal inferences:
898 haematology (non-count, non-percentage) subset.
- 899 • Figure S4. Significant (FDR <0.05) P2MR protein-outcome causal inferences:
900 anthropometric measurements subset.
- 901

902 **Figure 1.** Proteome-by-phenome Mendelian Randomisation (P²MR).

903 A) Genome-wide associations of the plasma concentrations of 249 proteins from two
904 independent European cohorts (discovery and replication) were calculated. The plot
905 shows pQTL position against chromosomal location of the gene that encodes the protein
906 under study for all replicated pQTLs. The area of a filled circle is proportional to its -
907 log₁₀(p-value) in the replication cohort. Blue circles indicate pQTLs ±150kb of the gene
908 ('local-pQTLs'); red circles indicate pQTLs more than 150kb from the gene. B, C) Local-
909 pQTLs of 64 proteins were taken forward for P²MR analysis. These were assessed against
910 778 outcome phenotypes from GeneAtlas (Canela-Xandri et al., 2017) (panel B; UK
911 Biobank) and 68 phenotypes identified using Phenoscanner (Staley et al., 2016) (panel C).
912 In each set of results an FDR of <0.05 was considered significant. D) Heterogeneity in
913 dependent instruments (HEIDI (Zhu et al., 2016)) testing was undertaken for MR
914 significant results from UK Biobank (n = 271). This test seeks to distinguish a single causal
915 variant at a locus effecting both exposure and outcome directly (as in i) or in a causal chain
916 (as in ii), from two causal variants in linkage disequilibrium (as in iii), one effecting the
917 exposure and the other effecting the outcome.

918

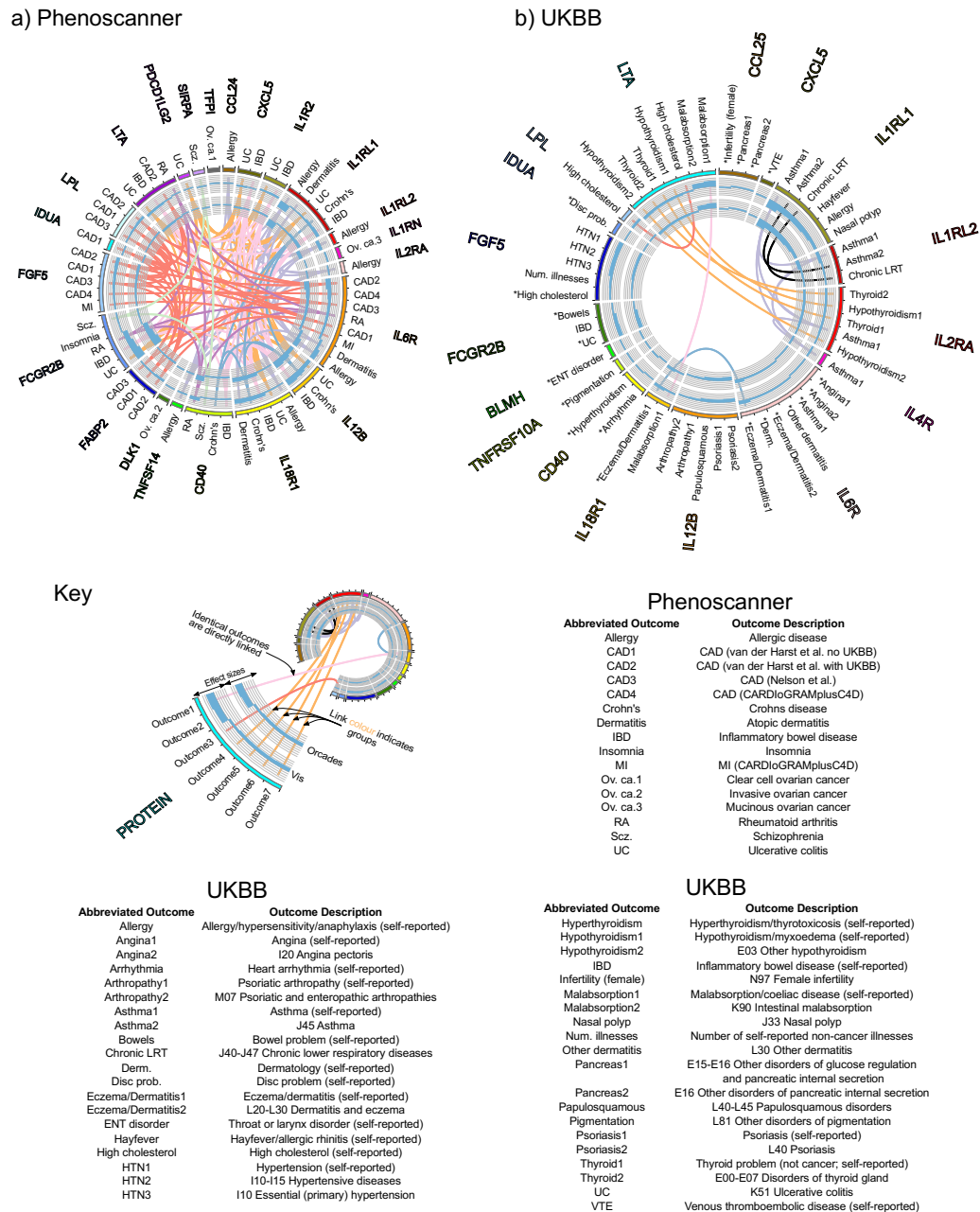
919 **Figure 1.**



920

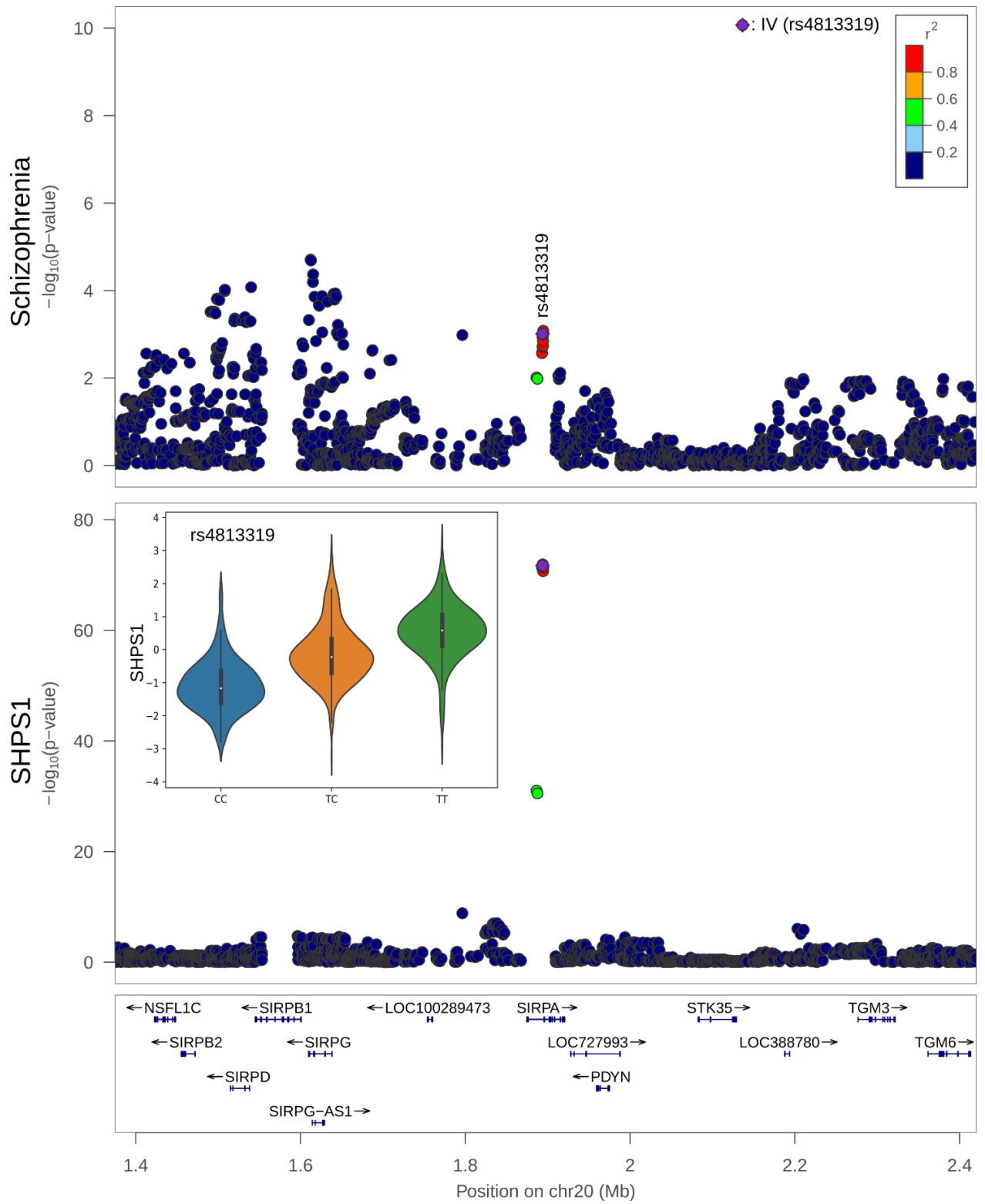
921 **Figure 2.** Significant (FDR <0.05) P²MR protein-outcome causal inferences: disease subset.
922
923 a) Phenoscanner (Staley et al., 2016): P²MR significant protein-disease outcome causal
924 inferences for 20 Phenoscanner studies. b) GeneAtlas (Canela-Xandri et al., 2017): MR
925 significant protein-disease outcome causal inferences for UK Biobank data. Asterisks
926 indicate P²MR estimates that are not significantly heterogeneous (HEIDI, Main Text (Zhu et
927 al., 2016)). Graphical key: Reading from the outside in: protein (exposure; HGNC symbol);
928 disease outcome; key colour; bar chart of the signed (beta/standard error)² value of the
929 MR estimate (using pQTL data from the discovery cohort; Methods); and bar chart of the
930 signed (beta/standard error)² value of the MR estimate (using pQTL data from the
931 replication cohort; Methods). Central chords join identical outcomes. Identically coloured
932 chords indicate similar outcome groups, e.g. thyroid disease.
933

934 **Figure 2**



936 **Figure 3: Co-localisation of SHPS1 (encoded by *SHPS1*: synonym *SIRPA*) and**
937 **schizophrenia DNA associations.** Upper panel, locuszoom (Pruim et al., 2010) of the region
938 surrounding *SHPS1* and the associations with schizophrenia (Schizophrenia Working Group
939 of the Psychiatric Genomics Consortium et al., 2014); lower panel, associations with SHPS1.
940 Lower panel inset, the relative concentration of SHPS1 across the 3 genotypes of rs4813319
941 – the DNA variant used as the instrumental variable (IV) in the MR analysis: CC, CT, and TT.
942

943 **Figure 3.**



945 **Supplementary Figure S1.** Significant (FDR <0.05) P²MR protein-outcome causal
946 inferences: haematology count subset.

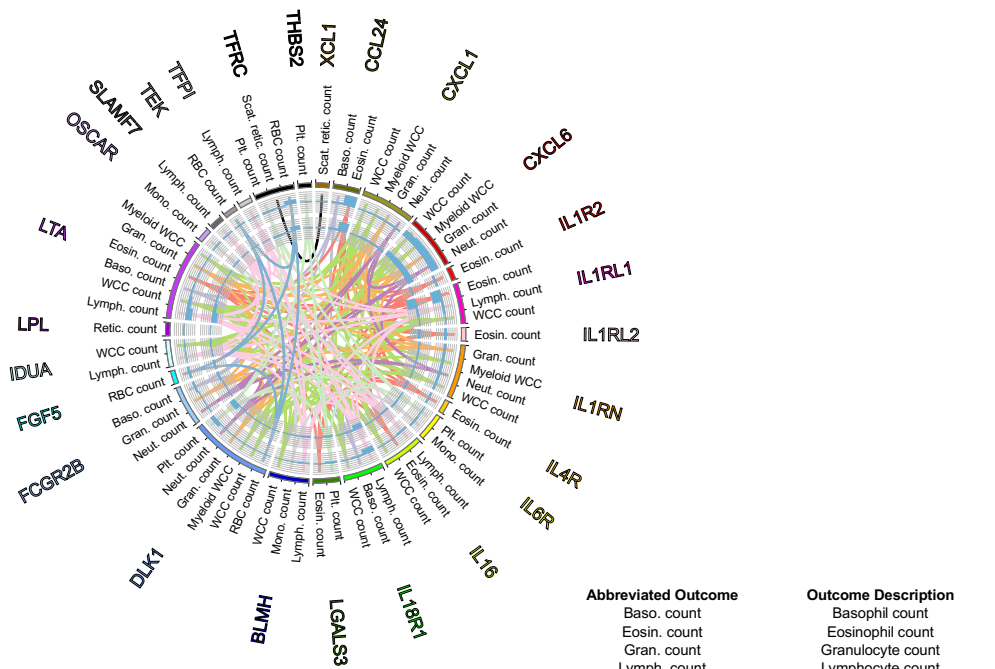
947 a) Phenoscanner (Staley et al., 2016): P²MR significant protein-haematology count outcome
948 causal inferences for 20 Phenoscanner studies. b) GeneAtlas (Canela-Xandri et al., 2017): MR
949 significant protein-haematology count outcome causal inferences for UK Biobank data.

950 Asterisks indicate P²MR estimates that are not significantly heterogeneous (HEIDI, Main
951 Text (Zhu et al., 2016)). Key as for Figure 2: Reading from the outside in: protein (exposure;
952 HGNC symbol); haematology count outcome; key colour; bar chart of the signed
953 (beta/standard error)² value of the MR estimate (using pQTL data from the discovery
954 cohort; Methods); and bar chart of the signed (beta/standard error)² value of the MR
955 estimate (using pQTL data from the replication cohort; Methods). Central chords join
956 identical outcomes. Identically coloured chords indicate similar outcome groups.

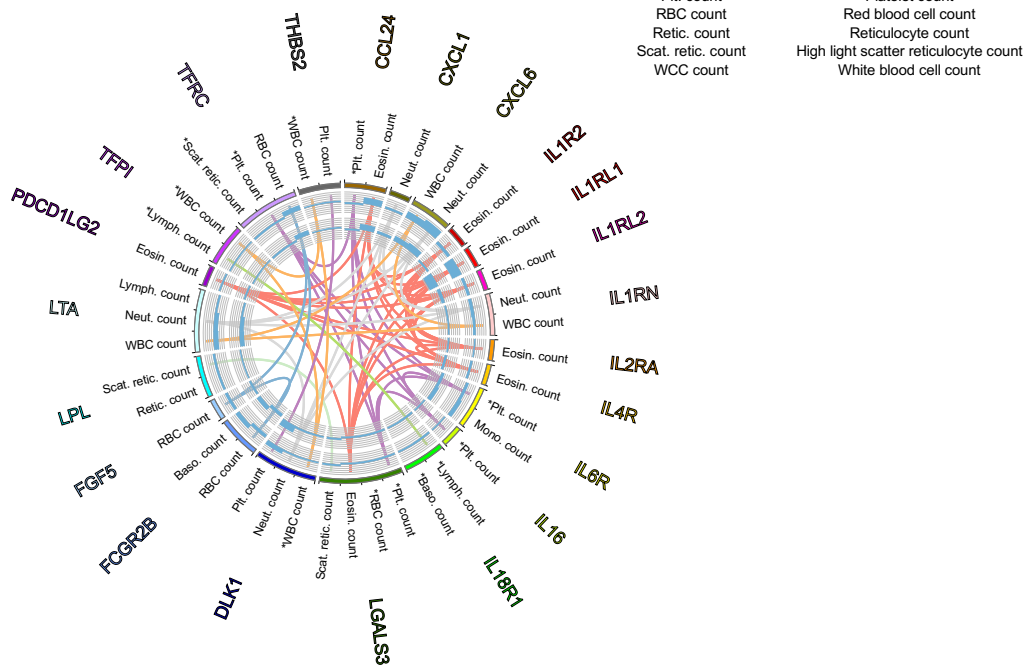
957

958 **Supplementary Figure S1.**

a) **Phenoscanner**



b) **UKBB**

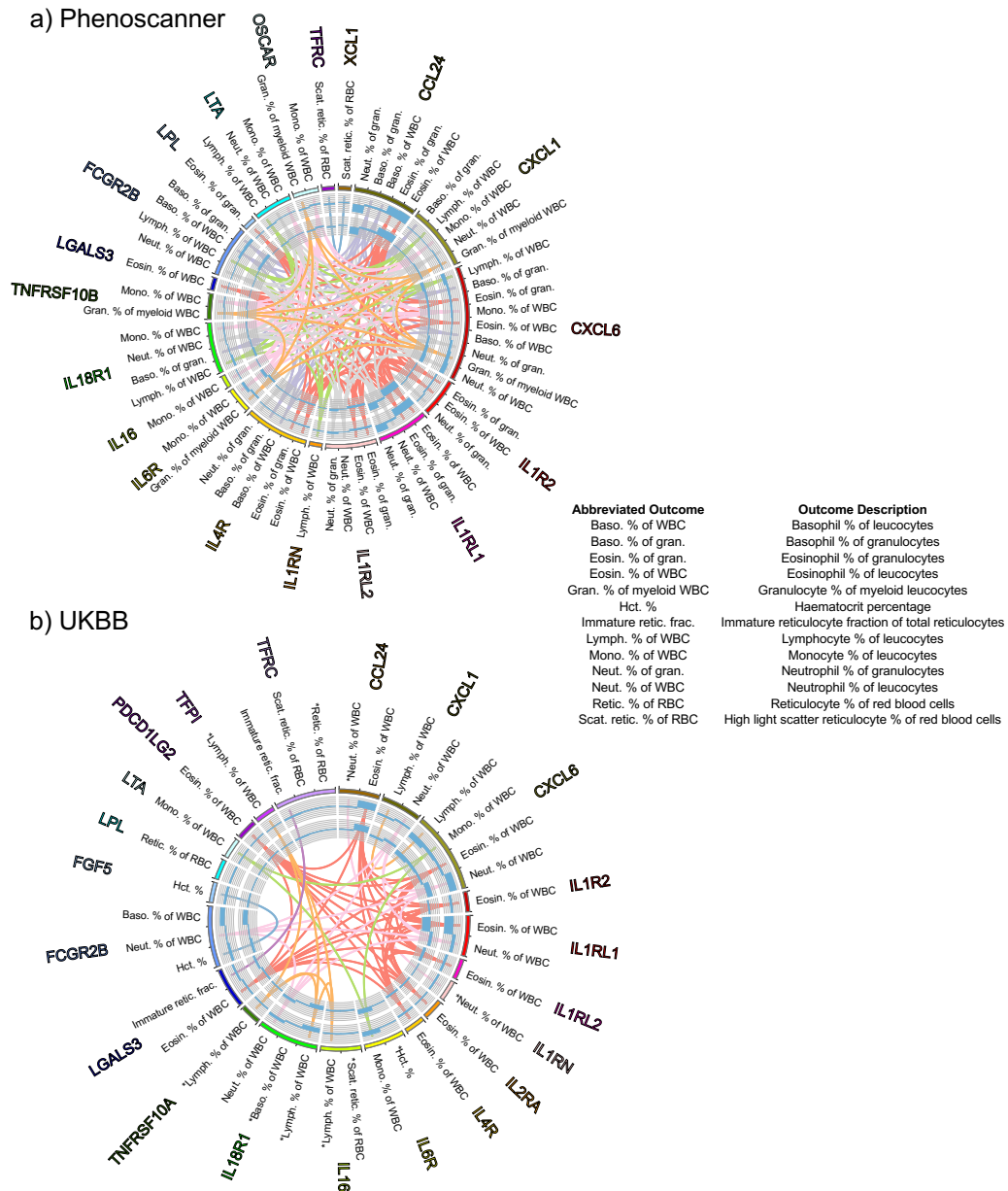


960 **Supplementary Figure S2.** Significant (FDR <0.05) P²MR protein-outcome causal
961 inferences: haematology percentage subset.

962 a) Phenoscanner (Staley et al., 2016): P²MR significant protein-haematology percentage
963 outcome causal inferences for 20 Phenoscanner studies. b) GeneAtlas (Canela-Xandri et al.,
964 2017): MR significant protein-haematology percentage outcome causal inferences for UK
965 Biobank data. Asterisks indicate P²MR estimates that are not significantly heterogeneous
966 (HEIDI, Main Text (Zhu et al., 2016)). Key as for Figure 2: Reading from the outside in:
967 protein (exposure; HGNC symbol); haematology percentage outcome; key colour; bar chart
968 of the signed (beta/standard error)² value of the MR estimate (using pQTL data from the
969 discovery cohort; Methods); and bar chart of the signed (beta/standard error)² value of the
970 MR estimate (using pQTL data from the replication cohort; Methods). Central chords join
971 identical outcomes. Identically coloured chords indicate similar outcome groups.

972

973 **Supplementary Figure S2.**



974 **Supplementary Figure S3.** Significant (FDR <0.05) P²MR protein-outcome causal
975 inferences: haematology (non-count, non-percentage) subset.

976 a) Phenoscanner (Staley et al., 2016): P²MR significant protein-haematology outcome causal
977 inferences for 20 Phenoscanner studies. b) GeneAtlas (Canela-Xandri et al., 2017): MR
978 significant protein-haematology outcome causal inferences for UK Biobank data. Asterisks
979 indicate P²MR estimates that are not significantly heterogeneous (HEIDI, Main Text (Zhu et
980 al., 2016)). Key as for Figure 2: Reading from the outside in: protein (exposure; HGNC
981 symbol); haematology outcome; key colour; bar chart of the signed (beta/standard error)²
982 value of the MR estimate (using pQTL data from the discovery cohort; Methods); and bar
983 chart of the signed (beta/standard error)² value of the MR estimate (using pQTL data from
984 the replication cohort; Methods). Central chords join identical outcomes. Identically
985 coloured chords indicate similar outcome groups.

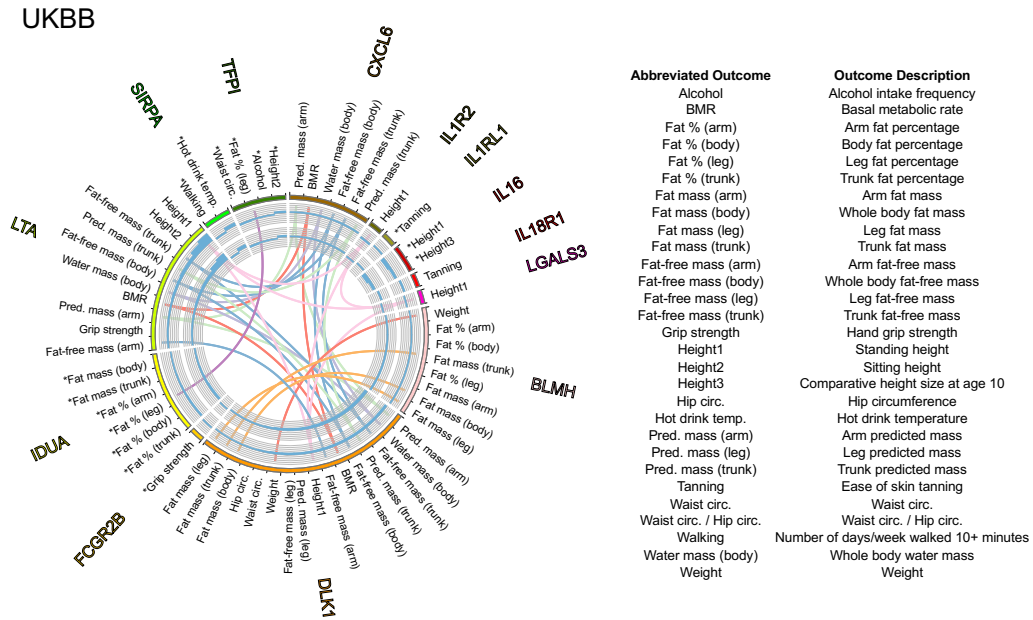
986

989 **Supplementary Figure S4.** Significant (FDR <0.05) P²MR protein-outcome causal
990 inferences: anthropometric measurements subset.

991 GeneAtlas (Canela-Xandri et al., 2017): MR significant protein-anthropometric
992 measurements outcome causal inferences for UK Biobank data. Asterisks indicate P²MR
993 estimates that are not significantly heterogeneous (HEIDI, Main Text (Zhu et al., 2016)). Key
994 as for Figure 2: Reading from the outside in: protein (exposure; HGNC symbol);
995 anthropometric measurements outcome; key colour; bar chart of the signed (beta/standard
996 error)² value of the MR estimate (using pQTL data from the discovery cohort; Methods); and
997 bar chart of the signed (beta/standard error)² value of the MR estimate (using pQTL data
998 from the replication cohort; Methods). Central chords join identical outcomes. Identically
999 coloured chords indicate similar outcome groups.

1000

1001 **Supplementary Figure S4.**



1002